# Journal of Nonlinear Sciences and Applications

# Hopf bifurcation control of calcium oscillations in hepatocytes

Quanbao Ji, Hongkun Zuo, Yi Zhou*

*School of Financial Science, Huainan Normal University, Huainan 232038, Anhui, P. R. China.*

Communicated by M. Bohner

## Abstract

This paper discusses a problem of the Hopf bifurcation control for a mathematical model of intracellular calcium oscillations by calculating the curvature coefficient of limit cycle and the bifurcation control theory. We find that the appearance and disappearance of calcium oscillations in this system are due to the supercritical and subcritical Hopf bifurcation of equilibrium points, respectively. In addition, a nonlinear feedback controller is proposed to control the frequency and amplitude of periodic orbits arising from the Hopf bifurcation. Numerical analysis and simulation results are carried out to illustrate the validity of the feedback controller in controlling Hopf bifurcations. ©2017 All rights reserved.

Keywords: Calcium oscillations, control, Hopf bifurcation, curvature coefficient.
2010 MSC: 37G10, 37J20.

## 1. Introduction

Free calcium ion is one of the important intracellular second messengers in living biological cells. Oscillations in concentration of calcium ions arise in response to extracellular agonist (neurotransmitter or hormone) and play a vital role in many cell types [1, 3, 5, 7, 8]. These calcium oscillations, such as spike, burst and chaos, were observed in a recent biological experiment on cultured cardiac myocytes [2]. A lot of mathematical models have been established to investigate the dynamical mechanism of these oscillatory activities. Among them, the model proposed by Kummer and co-workers considers that depending on the type of receptor, activation of Ga subunit of receptor complex could be self-enhanced. After binding of an agonist, Ga subunit of G proteins-coupled receptor is activated [4].

It is well-known that oscillatory activities may vary according to certain bifurcation principles and information is typically encoded in frequency, amplitude, and spatial calcium propagation. Therefore, numerical analysis and control of bifurcation are fundamental to study the appearance and disappearance of calcium oscillation in biological cells. The dynamical mechanisms of these calcium oscillations have been investigated both from theoretical and experimental points of view, over the past twenty years [6, 9–12].

---

*Corresponding author
*Email address:* zhouyi3280@163.com (Yi Zhou)

## 2. Model description

Towards a better understanding of the complex calcium oscillations in intracellular signal transduction, we take the model, proposed by Kummer et al., as an example of the Hopf bifurcation control systems of calcium oscillations. This model, which consists of three main variables: the free calcium concentration in the cytosol ($Ca_{cyt}$), the active PLC(PLC) and $G_\alpha$ subunit concentration ($G_\alpha$), is considered to preserve the above dynamics. The equations of this model are given as follows:

$$\begin{cases} dCa_{cyt}/dt = k_{10}G_\alpha - k_{11}\dfrac{Ca_{cyt}}{Ca_{cyt} + K_{12}}, \\ dG_\alpha/dt = k_1 + k_2 G_\alpha - k_3 PLC\dfrac{G_\alpha}{G_\alpha + K_4} - k_5 Ca_{cyt}\dfrac{G_\alpha}{G_\alpha + K_6}, \\ dPLC/dt = k_7 G_\alpha - k_8\dfrac{PLC}{PLC + K_9}. \end{cases} \tag{2.1}$$

Viewing $k_2$ as a bifurcation parameter, we study the existence and the stability of system (2.1) as $k_2$ is varied. Other parameters are: $k_1 = 0.212, k_3 = 1.52, k_5 = 4.88, k_7 = 1.24, k_8 = 32.24, k_{10} = 13.58, k_{11} = 153, K_4 = 0.19, K_6 = 1.18, K_9 = 29.09, K_{12} = 0.16$.

## 3. Main results

Let $x = Ca_{cyt}, y = G_\alpha, z = PLC, r = k_2$, we rewrite system (2.1) as:

$$\begin{cases} \dot{x} = 13.58y - 153x/(x + 0.16), \\ \dot{y} = ry - 4.88xy/(y + 1.18) - 1.52yz/(y + 0.19) + 0.212, \\ \dot{z} = 1.24y - 32.24z/(z + 29.09). \end{cases} \tag{3.1}$$

One can calculate the Jacobian matrix $(a_{ij})_{3\times3}$ of system (3.1), and get the following characteristic equation:

$$f(\lambda) = \lambda^3 + Q_1\lambda^2 + Q_2\lambda + Q_3,$$

where

$$Q_1 = -(a_{11} + a_{22} + a_{33}),$$
$$Q_2 = a_{11}a_{22} + a_{11}a_{33} + a_{22}a_{33} - a_{13}a_{31} - a_{12}a_{21} - a_{32}a_{23},$$
$$Q_3 = a_{31}a_{13}a_{22} + a_{12}a_{21}a_{33} + a_{32}a_{23}a_{11} - a_{11}a_{22}a_{33} - a_{12}a_{23}a_{31} - a_{13}a_{21}a_{32}.$$

After a simple computation, we get the following conclusions:

(1) system (3.1) has a stable node when $r < 1.316$;

(2) system (3.1) has a non-hyperbolic equilibrium point $O_1 = (0.0158, 1.013, 1.1793)$ when $r = 1.316$;

(3) system (3.1) has an equilibrium point (saddle) when $1.316 < r < 2.999$;

(4) system (3.1) has a non-hyperbolic equilibrium point $O_2 = (0.8617, 9.5022, 16.7551)$ when $r = 2.999$;

(5) system (3.1) has a stable node when $r > 2.999$.

For $r = 1.316$ we consider the equilibrium point $O_1$ and calculate the eigenvalues of system (3.1) at $(0.0158, 1.013, 1.1793)$. Then

$$\alpha'(1.316) = \text{real}\left(\frac{\partial\alpha(r)}{\partial r}|_{r=1.316}\right) = \text{real}\left(-\frac{f_r'(\lambda)}{f_\lambda'(\lambda)}\right) = 0.5003.$$

Fig. 1 displays the bifurcation diagram of the equilibrium points of system (3.1). Each point of the curve (solid line) denotes the stable equilibrium points, and the dashed line indicates unstable equilibrium points. Filled circles represent stable periodic orbits and open circles are unstable. It is seen that the equilibrium undergoes two bifurcation points (HB1 and HB2). Corresponding parameter values are $k_2^1 = 1.316$ and $k_2^2 = 2.999$, respectively. When $k_2 < k_2^1$, there exists a stable equilibrium point of system (3.1). As $k_2$ increases, the equilibrium point loses its stability at HB1, and returns to be stable at HB2.
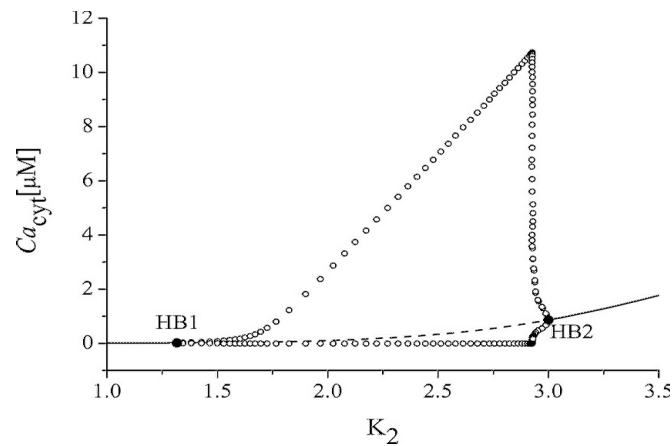


Figure 1: Equilibrium curve of (3.1) in $(k_2, Ca_{cyt})$ plane.

Suppose

$$\begin{pmatrix} x \\ y \\ z \end{pmatrix} = \begin{pmatrix} 0.0158 \\ 1.013 \\ 1.1793 \end{pmatrix} + P \begin{pmatrix} u \\ v \\ w \end{pmatrix},$$

where

$$P = \begin{pmatrix} 0 & 1 & 1 \\ 0.0541 & 58.3276 & 0.0028 \\ -33.4393 & 46.6649 & -0.000004455 \end{pmatrix}.$$

Hence

$$\begin{pmatrix} \dot{u} \\ \dot{v} \\ \dot{w} \end{pmatrix} = \begin{pmatrix} 0 & -0.7348 & 0 \\ 0.7348 & 0 & 0 \\ 0 & 0 & -791.9855 \end{pmatrix} \cdot \begin{pmatrix} u \\ v \\ w \end{pmatrix} + \begin{pmatrix} Q_1 \\ Q_2 \\ Q_3 \end{pmatrix},$$

where

$Q_1 = 0.355789v - 0.000352u - 0.000018w + 0.962889a + 0.010257b - 0.116611c + 0.036321d - 0.001517,$

$Q_2 = 1.278389v - 0.733614u + 0.000061w - 0.000893a + 0.007336b - 0.083561c + 0.026027d + 0.025832,$

$Q_3 = 790.8104v + 0.733492u + 792.023w + 0.000893a - 153.0073b + 0.083561c - 0.026027d + 13.7307,$

$$a = \frac{\sigma_1 - 1.1793}{\sigma_1 - 30.2693}, \quad b = \frac{v + w + 0.0158}{v + w + 0.1758}, \quad c = \frac{(v + w + 0.0158)(\sigma_2 + 1.013)}{(\sigma_2 + 2.193)}, \quad d = \frac{(\sigma_1 - 1.1793)(\sigma_2 + 1.013)}{\sigma_2 + 1.203},$$

$\sigma_1 = 33.4393u - 46.6649v + 0.000004455w, \quad \sigma_2 = 0.0541u + 58.3276v + 0.0028w.$

To facilitate the following discussion, we do the following hypotheses:

$$(t_1, t_2, t_3) = (u, v, w), \quad L_{jk}^i = \frac{\partial Q_i}{\partial t_j \partial t_k}\bigg|_{(t_1,t_2,t_3,r)=(0,0,0,1.316)}, \quad L_{jks}^i = \frac{\partial Q_i}{\partial t_j \partial t_k \partial t_s}\bigg|_{(t_1,t_2,t_3,r)=(0,0,0,1.316)}.$$

One can calculate the following characteristic quantities for $r = 1.316$ and $(u, v, w) = (0, 0, 0)$,

$$g_{20} = 0.25(L_{11}^1 - L_{22}^1 + 2L_{12}^2 + i(L_{11}^2 - L_{22}^2 - 2L_{12}^1)),$$

$$g_{11} = 0.25(L_{11}^1 + L_{22}^1 + i(L_{11}^2 + L_{22}^2)),$$
$$G_{110} = 0.5(L_{13}^1 + L_{23}^2 + i(L_{13}^2 - L_{23}^1)),$$
$$G_{101} = 0.5(L_{13}^1 - L_{23}^1 + i(L_{13}^2 + L_{23}^1)),$$
$$w_{11} = \frac{1}{4 \times 791.9855}(L_{11}^3 + L_{22}^3),$$
$$w_{20} = \frac{1}{4 \times (2 \times 0.7348i + 791.9855)} \cdot (L_{11}^3 - L_{22}^3 - 2iL_{12}^3),$$
$$G_{21} = \frac{1}{8}(L_{111}^1 + L_{122}^1 + L_{112}^2 + L_{222}^2 + i(L_{111}^2 + L_{122}^2 - L_{112}^1 - L_{222}^1)).$$

After the computation, we have

$$g_{20} = 3.049079 - 3.92752i, \quad g_{11} = -0.832716 + 0.59769i, \quad\quad\quad G_{110} = -0.814186 + 1.135644i,$$
$$G_{101} = 0.813086 - 1.136432i, \quad w_{11} = 2.843756, \ w_{20} = -2.843748 + 0.00949i, \quad G_{21} = -177.3318 + 1.155082i.$$

Then the curvature coefficient of limit cycle is described by

$$\sigma = \text{Re}\left\{ \frac{g_{20}g_{11}}{2 \times 0.7348}i + G_{110}w_{11} + \frac{G_{21} + G_{101}w_{20}}{2} \right\} = -95.5975.$$

For $| r - 0.2345 | \ll 1$, the amplitude of limit cycle of (3.1) is

$$R \ll \sqrt{-\frac{\alpha'(1.316)}{\sigma}(r - 1.316)} = 0.0515\sqrt{r - 1.316}.$$

Summarizing the discussion above, we draw the following conclusion based on the Hopf bifurcation theory:

**Conclusion 3.1.** A supercritical Hopf bifurcation occurs when r passes through $r_0 = 1.316$ of system (3.1). When $r < r_0$, the equilibrium point $O_1$ is stable. When $r > r_0$, the equilibrium point $O_1$ will lose its stability, meanwhile the neighborhood around it has a stable periodic solution and the (3.1) begins to oscillate.

For $r_0 = 2.999$, the characteristic roots of equilibrium point $O_2 = (0.8617, 9.5022, 16.7551)$ of (3.1) are $\xi_1 = -20.9912, \xi_2 = 1.3674i, \xi_3 = C1.3674i$, respectively.

$$\alpha'(2.999) = \text{real}\left( \frac{\partial\alpha(r)}{\partial r}|_{r=2.999} \right) = \text{real}\left( -\frac{f'_r(\lambda)}{f'_\lambda(\lambda)} \right) = 0.55703.$$

Then the curvature coefficient of limit cycle is described by

$$\sigma = \text{Re}\left\{ \frac{g_{20}g_{11}}{2 \times 1.3674}i + G_{110}w_{11} + \frac{G_{21} + G_{101}w_{20}}{2} \right\} = -0.7892,$$

where

$$g_{20} = 0.615496 + 1.322315, \quad g_{11} = -0.627172 - 1.322487i, \quad\quad\quad G_{110} = -2.63636 + 1.23378,$$
$$G_{101} = 2.635154 - 1.236266i, \quad w_{11} = 0.609733, \ w_{20} = -0.599604 + 0.078183i, \quad G_{21} = 1.918087 - 0.900265i.$$

Conclusion 3.2 can be inferred when $\alpha'(2.999) > 0$ and $\sigma < 0$.

**Conclusion 3.2.** A subcritical Hopf bifurcation occurs when r passes through $r_0 = 2.999$ of system (3.1). When $r < r_0$, the equilibrium point $O_2$ is unstable, and system (3.1) is going to oscillate. However, when $r > r_0$, the equilibrium point $O_2$ is stable, and oscillatory phenomena of system (3.1) disappear.

Next, a nonlinear feedback controller is introduced to avoid re-computing values of the equilibrium points and the Hopf bifurcation points of (3.1). We therefore assume the suitable controller form given by:

$$U(X, r) = \begin{bmatrix} k(y - 9.5022)^2 & 0 & 0 \end{bmatrix}^T.$$

We have the following control system by adding the above term on the right of the first equation of system (3.1):

$$\begin{cases} dCa_{cyt}/dt = k_{10}G_\alpha - k_{11}\dfrac{Ca_{cyt}}{Ca_{cyt} + K_{12}} + k(y - 9.5022)^2, \\[2mm] dG_\alpha/dt = k_1 + k_2G_\alpha - k_3PLC\dfrac{G_\alpha}{G_\alpha + K_4} - k_5Ca_{cyt}\dfrac{G_\alpha}{G_\alpha + K_6}, \\[2mm] dPLC/dt = k_7G_\alpha - k_8\dfrac{PLC}{PLC + K_9}. \end{cases} \tag{3.2}$$

According to the analysis of amplitude of limit cycle, we get

$$\begin{pmatrix} \dot{u} \\ \dot{v} \\ \dot{w} \end{pmatrix} = \begin{pmatrix} 0 & -1.3674 & 0 \\ 1.3674 & 0 & 0 \\ 0 & 0 & -20.9912 \end{pmatrix} \cdot \begin{pmatrix} u \\ v \\ w \end{pmatrix} + \begin{pmatrix} \widetilde{Q}_1 \\ \widetilde{Q}_2 \\ \widetilde{Q}_3 \end{pmatrix},$$

where

$$\begin{pmatrix} \widetilde{Q}_1 \\ \widetilde{Q}_2 \\ \widetilde{Q}_3 \end{pmatrix} = \begin{pmatrix} Q_1 \\ Q_2 \\ Q_3 \end{pmatrix} + \begin{pmatrix} U_1 \\ U_2 \\ U_3 \end{pmatrix}, \quad \begin{pmatrix} U_1 \\ U_2 \\ U_3 \end{pmatrix} = \begin{pmatrix} -0.0533 & 0.2522 & -0.7020 \\ -0.1136 & 0.6304 & 0.0457 \\ 1.1136 & -0.6304 & -0.0457 \end{pmatrix} \cdot U(X, r).$$

Similar to our previous analysis, it is concluded that

$$\widetilde{g}_{20} = g_{20} + k(0.0595 + 0.1885i), \qquad \widetilde{g}_{11} = g_{11} - k(0.0798 + 0.1699i),$$
$$\widetilde{G}_{110} = G_{110} - k(0.0365 - 0.0146i), \qquad \widetilde{G}_{101} = G_{101} + k(0.0345 - 0.0187i),$$
$$\widetilde{w}_{11} = w_{11} + 0.0794k, \qquad \widetilde{w}_{20} = w_{20} + k(-0.0787 + 0.00103i), \quad \widetilde{G}_{21} = G_{21}.$$

When $| r - 2.999 | \ll 1$, the curvature coefficient of limit cycle is described by

$$\widetilde{\sigma} = \text{Re}\left\{ \frac{\widetilde{g}_{20}\widetilde{g}_{11}}{2 \times 1.3674}i + \widetilde{G}_{110}\widetilde{w}_{11} + \frac{\widetilde{G}_{21} + \widetilde{G}_{101}\widetilde{w}_{20}}{2} \right\}$$
$$= \sigma + \text{Re}\left\{ k^2(0.00495 + 0.01189i) + k(-0.19535 + 0.30554i) \right\}$$
$$= 0.00495k^2 - 0.19535k - 0.78924.$$

The amplitude of limit cycle of system (3.2) is given as

$$\widetilde{R} \ll \sqrt{-\frac{\alpha'(2.999)}{\sigma}(r - 2.999)}.$$

Furthermore, defining $P = \dfrac{R}{\widetilde{R}}$, then we have

$$P = \sqrt{1 + 0.1061k - 0.6537k^2}.$$

Hopf bifurcation control can be accomplished in the range $-1.1554 < k < 1.3169$ of the control parameter $k$ under appropriate conditions. The goal is to indirectly change the value of $P$, thereby controlling the frequency and amplitude of the limit cycles.

In order to illustrate the effectiveness of the proposed method, we now choose the control parameters $k = 1.29$ and $K_2 = 2.05$. Fig. 2 shows the manipulation of frequency and amplitude of calcium oscillation. Fig. 2 (a) is the above oscillation behavior with parameters $K_2 = 2.05$ and $k = 0$. The corresponding phase portraits is also plotted in Fig. 2 (c). Fig. 2 (b) is the control oscillation with parameters $K_2 = 2.05$ and $k = 1.29$. The corresponding phase portraits is plotted in Fig. 2 (d). One can observe that an increase of the control parameter $k$ correlates with reduction of the frequency and amplitude of the above calcium oscillations.
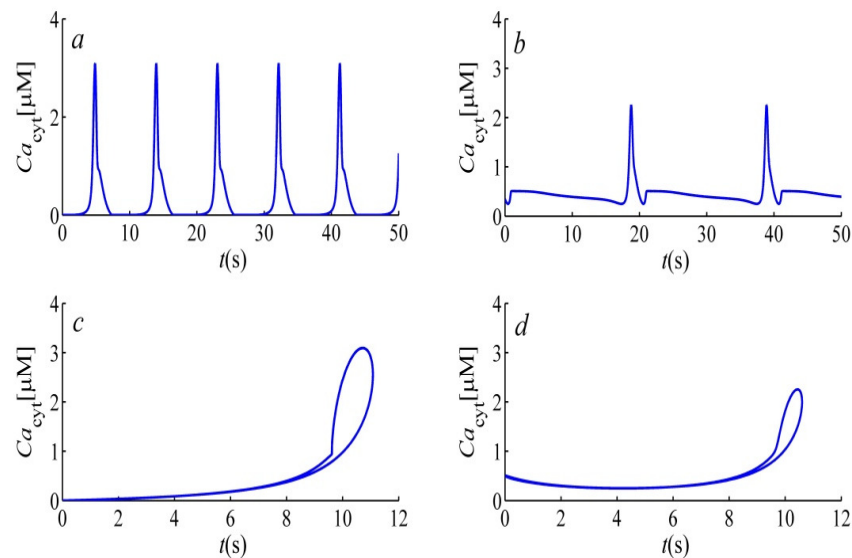


Figure 2: Comparison of frequency and amplitude manipulation of calcium oscillation for $K_2 = 2.05$. (a) Time series for $k = 0$. (b) Time series under control for $k = 1.29$. (c) Corresponding phase portraits for $k = 0$. (d) Phase portraits under control for $k = 1.29$.
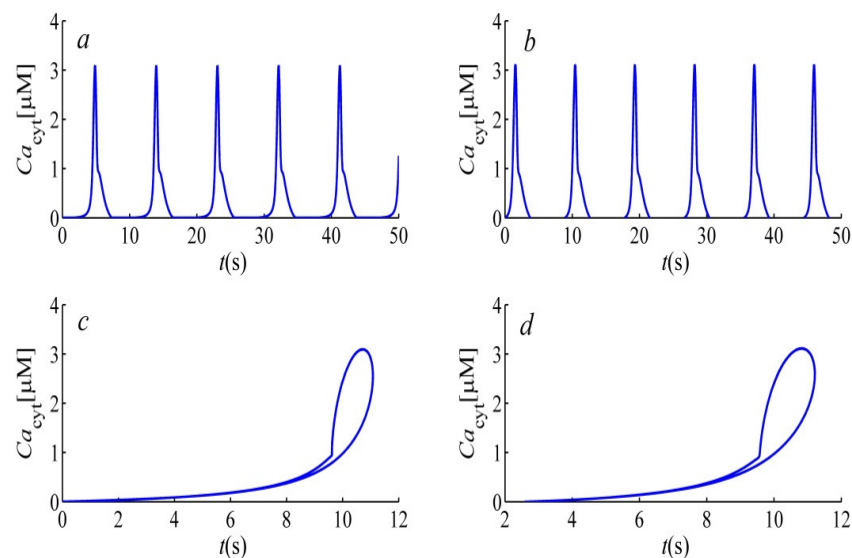


Figure 3: Comparison of frequency and amplitude manipulation of calcium oscillation for $K_2 = 2.05$. (a) Time series for $k = 0$. (b) Time series under control for $k = -0.802$. (c) Corresponding phase portraits for $k = 0$. (d) Phase portraits under control for $k = -0.802$.

Unlike the previous case, we consider an increased frequency of calcium waves. For this purpose, we

choose $k = -0.802$ and $K_2 = 2.05$. Fig. 3 (a) and (c) in left column are the same to Fig. 2. Fig. 3 (b) and (d) are the control oscillation with parameter $k = -0.802$. It is seen that an increase in number of spikes in Fig. 3 (b) with varying the control parameter. Fig. 3 (d) is the corresponding phase portrait and incorporates the manipulation of amplitude of spike.

## 4. Conclusion

In this article, we study the frequency and amplitude control problem of Hopf bifurcation in a mathematical model proposed by Kummer et al. under a nonlinear feedback controller. It is shown that the supercritical and subcritical Hopf bifurcations play a vital role in occurrence of calcium oscillations. Explicit control formula and amplitude approximation are given by calculating the curvature coefficient of limit cycle. In addition, numerical simulations are drawn and verified the manipulation of frequency and amplitude of intracellular calcium oscillations by changing the control parameter.

## Acknowledgment

## References

[1] M. Berridge, G. Dupont, *Spatial and temporal signalling by calcium*, Curr. Opin. Cell Biol., **6** (1994), 267–274. 1

[2] H.-G. Gu, B.-B. Pan, G.-R. Chen, L.-X. Duan, *Biological experimental demonstration of bifurcations from bursting to spiking predicted by theoretical models*, Nonlinear Dynam., **78** (2014), 391–407. 1

[3] H.-G. Gu, B.-B. Pan, J. Xu, *Experimental observation of spike, burst and chaos synchronization of calcium concentration oscillations*, Europhys. Lett., **106** (2014), 6 pages. 1

[4] U. Kummer, L. F. Olsen, C. J. Dixon, A. K. Green, E. Bornberg-Bauer, G. Baier, *Switching from simple to complex oscillations in calcium signaling*, Biophys. J., **79** (2000), 1188–1195. 1

[5] Q.-S. Lu, H.-G. Gu, Z.-Q. Yang, X. Shi, L.-X. Duan, Y.-H. Zheng, *Dynamics of firing patterns, synchronization and resonances in neuronal electrical activities: experiments and analysis*, Acta Mech. Sinica, **24** (2008), 593–628. 1

[6] Y. Lu, Q.-B. Ji, *Control of intracellular calcium bursting oscillations using method of self-organization*, Nonlinear Dynam., **67** (2012), 2477–2482. 1

[7] M. Marhl, T. Haberichter, M. Brumen, R. Heinrich, *Complex calcium oscillations and the role of mitochondria and cytosolic proteins*, Biosyst., **57** (2000), 75–86. 1

[8] M. Perc, M. Marhl, *Different types of bursting calcium oscillations in non-excitable cells*, Chaos Solitons Fractals, **18** (2003), 759–773. 1

[9] C. C. Santini, A. M. Tyrrell, *The manipulation of calcium oscillations by harnessing self-organisation*, Biosyst., **94** (2008), 153–163. 1

[10] S. Schuster, M. Marhl, T. Hofer, *Modelling of simple and complex calcium oscillations*, Eur. J. Biochem., **269** (2002), 1333–1355.

[11] J.-S. Tang, Z.-L. Chen, *Amplitude control of limit cycle in van der Pol system*, Internat. J. Bifur. Chaos Appl. Sci. Engrg., **16** (2006), 487–495.

[12] N. M. Woods, K. R. Cuthbertson, P. H. Cobbold, *Repetitive transient rises in cytoplasmic free calcium in hormone-stimulated hepatocytes*, Nature, **319** (1986), 600–602. 1